

Synthesis, Spectroscopic, and Characterization of Novel Nano Sized Mannich Base Complexes with Pt (IV) and Au (III) Ions and Assessing Their Antioxidants Activity

Alya'a J. Ahmed ¹, Mahasin F. Alias ²

¹ Ministry of Higher Education and Scientific Research, Baghdad, Iraq

² Department of Chemistry, College of Science for Women, University of Baghdad, Baghdad, Iraq.

*Corresponding Author.

Received 08/02/2023, Revised 20/06/2023, Accepted 22/06/2023, Published Online First 20/03/2024,
Published 01/10/2024



© 2022 The Author(s). Published by College of Science for Women, University of Baghdad.

This is an open-access article distributed under the terms of the [Creative Commons Attribution 4.0 International License](https://creativecommons.org/licenses/by/4.0/), which permits unrestricted use, distribution, and reproduction in any medium, provided the original work is properly cited.

Abstract

This study focuses on the synthesis of nano pt(IV) and Au(III) Mannich base complexes derived from ciprofloxacin by the ultrasonic sonication method. The size and morphology of nanocomplex were measured by transmission electron microscopy (TEM), atomic force microscopy (AFM), energy dispersive X-ray (EDX), scanning electron microscopy (SEM), x-ray diffraction (XRD) and Fourier transform infrared spectroscopy (FTIR). Newly synthesized ligand and their metal complexes were tested for their ability to scavenge free radicals at concentrations between 6.25 and 100 µg/ml using their interaction with the stable free radical 1,1-diphenyl-2-picrylhydrazyl (DPPH). It has been demonstrated that all compounds enhance antioxidant activity in high concentration.

Keywords: Antioxidant, Ciprofloxacin, Free radicals, Mannich base complexes, Nano size.

Introduction

Free radicals were implicated within side the causation of numerous oxidative damage diseases including liver cirrhosis, atherosclerosis, cancer, diabetes, and ageing¹. Antioxidants are our body's first line of defense against free radical damage. As our exposure to free radicals increases due to pollution, cigarette smoke, medications, illness, stress, or even exercise, the need for antioxidants becomes even more critical². Scavenging efficacy of numerous organic compounds may be evaluated utilizing DPPH free radical, and additionally (2,2'-azino-bis(3-ethylbenzothiazoline-6-sulfonate) ABTS⁺ tests. Many organic molecules have already been notified that act as antioxidants are very good, so it's far paramount to recognize the approach of motion as the proper efficacy of these antioxidants. There are large numbers of normal and properly

artificial anti-oxidants that will be explored; additionally, their antioxidant capacity can be evaluated in different ways³. The compounds derived from the Mannich base reaction had been implicit supply to inhibit pathogens with much fewer side effects⁴. The electron-withdrawing substituents confirmed much less activity than electron-donating substituents towards microorganisms^{5, 6}. Mannich base complexes have remained a critical and popular area of study because of their easy synthesis, adaptability, and various variety of applications⁷. In recent years, metal complexes with quinoline derivatives have been shown to have possible antibacterial activity as well as antioxidant activity⁸. A novel unexplored field of research is the production of transition-metal complexes with close attention to biological processes. Additionally, it is a

popular area of study to use DFT simulations and molecular docking research to determine the method of the pharmacological action and the effectiveness of therapeutic agents⁹. Recent studies have discovered different forms of antioxidant tendency. Nano-antioxidants have been prepared using a variety of materials, metal and metal oxide nanoparticles, CNTs, other carbonaceous nanomaterials and Polymer-loaded antioxidant nanoparticles have been reported to possess antioxidant function. Various forms of antioxidant have recently been discovered

research trends. Biodegradable nanoparticles have received a lot of attention recently. Due to its high encapsulation efficiency, controlled release properties and non-toxicity, among other factors. As a carrier for various forms of nano-antioxidants historically, biodegradable polymers have proven to be the most important materials to investigate^{10, 11}. Uses metallic nanoparticles with high antioxidant activity develop new antioxidants.

Materials and Methods

The chemicals and reagents that were used for this study are Ciprofloxacin (99.5%), 2-mercaptobenzimidazole, metals chloride, methanol, ethanol, formaldehyde, and 2,2-diphenyl-1-picrylhydrazyl (DPPH); all chemical reagents were of analytical grade and used without further purification. The energy dispersive X-ray (EDX) and field emission scanning electron microscopy (FESEM) images were recorded using a Tescan MIRA3 LMU instrument (Tescan Orsay Holding; Brno-Kohoutovice, Czech Republic). The Agilent spectrometer (FT-IR 8400S SHIMADZU Spectrophotometer) was used to measure FTIR spectra of prepared complexes and their ligand in the solid-state at the range of wavenumber at 4000-400 & 4000-200 cm^{-1} using KBr & CsI pellets. Whereas the powder XRD data were recorded on a diffractometer (X-ray tube target: $\text{CuK}\alpha$ ($\lambda = 1.5406$ nm)). The AFM measurements were recorded by the instrument Veeco's Atomic Force Microscope and Transmission electron microscope (TEM) type JEOL-(JEM)-2100.

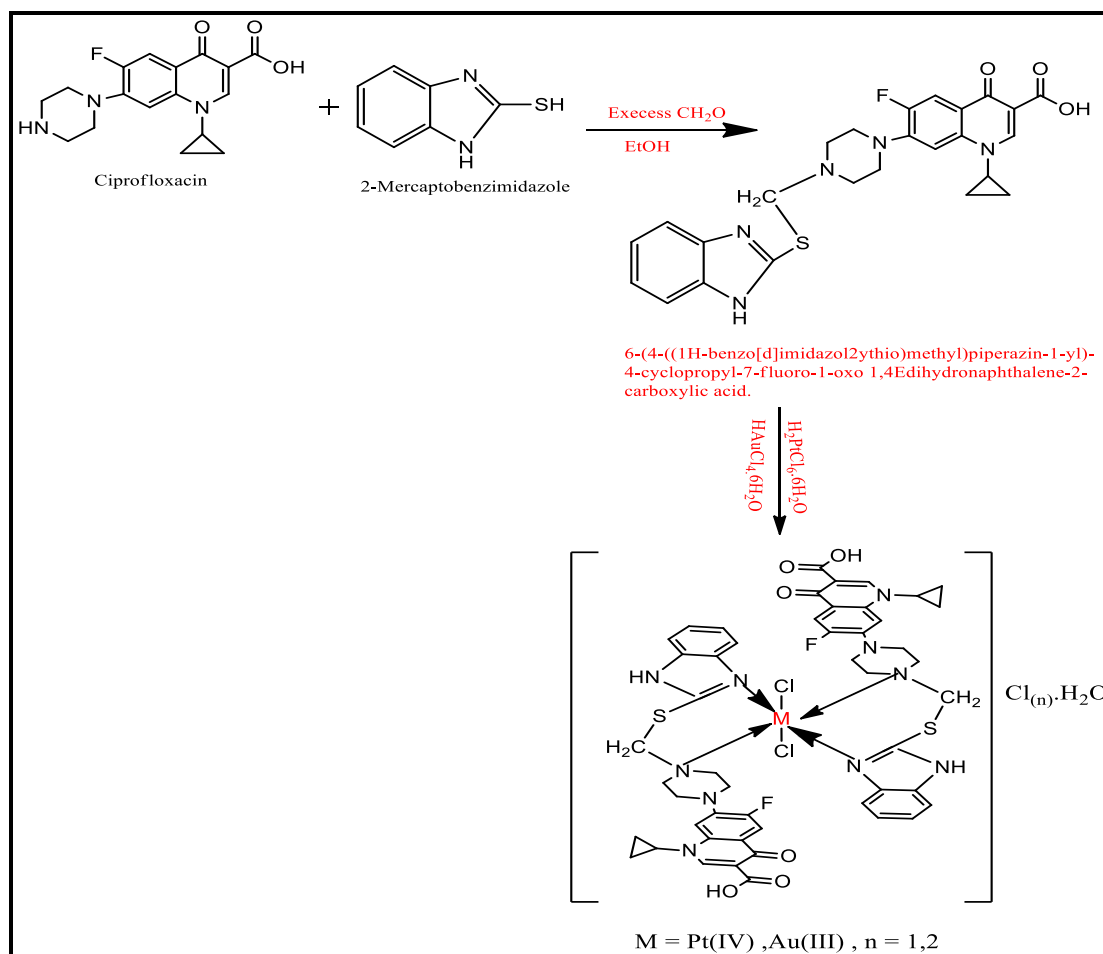
Synthesis of Mannich Base Ligand

General procedure for the preparation of ligand (CPFX, 1.65 g, 0.005 mol) and 2-

mercaptobenzimidazole (0.75 g, 0.005 mol) in EtOH (25 mL). A solution (CH_2O) was applied and heated to reflux for 6 hours and cooled to room temperature. The precipitate was filtered and recrystallized from (ethanol in water) to give the compound¹².

Synthesis of Nanocomplex

The desired metal ion was mixed with 2mmoles of Mannich base (L) that have been dissolved in 10ml of absolute ethanol (0.409g $\text{H}_2\text{PtCl}_6 \cdot 6\text{H}_2\text{O}$ and 0.354g $\text{HAuCl}_4 \cdot 6\text{H}_2\text{O}$). The mixture was refluxed for two hours, changing the color. After the solvent evaporated the resultant precipitates were created. The precipitates were then dried to produce the metal complexes. Then, 0.125 g of the metal complexes were individually dissolved in water (50 mL). The mixture of the solution was exposed to ultrasonic sonication for two hours at 60 °C. After overnight incubation at room temperature, crystals of good quality began to form. Novel compounds were then isolated by filtration.



Schem 1. Synthesis of Mannich base ligand and its metal complexes.

Antioxidant Activity

The stable free radical 2,2-diphenyl-1-picrylhydrazyl (DPPH) technique was used to test the synthesized compound's antioxidant activity. The samples were first diluted in methanol to various concentrations (6.25,

12.5, 25, 50, and 100 µg/ml), and then 0.3 mL of each concentration solution was combined with 2.7 mL of a methanol solution containing DPPH radicals. The combination was left at room temperature and in the dark for 60 minutes. A UV-Vis spectrophotometer was used to measure the absorbance at 517 nm to detect DPPH radical scavenging. For each

concentration, the average of three separate replications was used to calculate all values. The formula was used to determine the antioxidant capacity using ascorbic acid as the standard (positive control)¹³ in Eq. 1.

$$I\% = \frac{Abs\ blank - Abs\ sample}{Abs\ blank} \times 100 \dots \dots \dots 1$$

Where the Abs sample is the test compound and Abs blank is the absorbance of the control reaction, which contains all of the reagents but not the test compound. Plotting the proportion of DPPH-scavenging activity versus sample concentration was done to calculate the IC 50, which is the absorbance of values for each synthesized compound.

Results and Discussion

Structural Characterizations

As predicted, FTIR provided useful information concerning the interactions between the ligand and

Pt⁴⁺ and Au³⁺ ions. When compared to literature values, the characteristic frequencies of the free ligand and its metal complexes were easily assigned¹⁴ The FTIR spectrum of the ligand Fig. 1 is

complicated due to the large number of groups which have overlapping regions, however a few the bands are selected in order to prove the complexation. Table 1 lists the principal IR bands of the free ligand and its metal complexes. The spectrum of ligand shows stretching frequency of $\nu(\text{CH}_2\text{-N})$, $\nu(\text{C}=\text{N})$, at 2964-2839, 1552, cm^{-1} respectively, the other bands appeared at 3531,1708,1627,1051,1361,1271,1137,738 cm^{-1} are assigned to stretching frequency of ν OH of COOH group, ν C=O, ν NCS, ν NCN, ν CNC, ν CSC, and ν CS respectively. The FTIR spectrum of the Pt(IV) nano complex, Fig. 2 shows, the frequencies at 1707 cm^{-1} and 1627 cm^{-1} , respectively, are ascribed to the $\nu(\text{C}=\text{O})$ of the carboxylic and carbonyl groups. In comparison to the free ligand, these vibration bands occur at the same frequencies (1708 cm^{-1} and 1627 cm^{-1}). These results showed that no carboxylic and carbonyl groups of oxygen atoms participated in the coordination of metal ions. In Infrared spectra of complexes, the ν NH, bands did not change in

intensity and position when comparing the same bands of the ligand, this proves the amine does not coordinate. The bands which were attributed to the $\nu(\text{CH}_2\text{-N})$ of the ligand mentioned previously were shifted to higher wave numbers in both complexes about (6-15) and (1-13) cm^{-1} , while the band which to the $\nu(\text{C}=\text{N})$ of imidazole ring shifted to lower wave number in both complexes about (9-44) cm^{-1} as shown in Table 1. This indicates that the ligand acts as a neutral bidentate through the N atom of Mannich base and the N atom of the imidazole ring. The weak absorption bands present at frequencies below 500 cm^{-1} are assigned to the coordination bonds $\nu(\text{M-N})^{15}$ between a metal ion and nitrogen atom of Mannich base derivative from ciprofloxacin. The complexes spectra exhibited new weak bands at a frequency range (345-352) cm^{-1} assigned to the stretching frequency of (M-Cl)¹⁶ for Pt(IV) and Au(III) complexes. Bands appeared in two complexes varying between 3442-3450 cm^{-1} which refer to stretching band of water uncoordination¹⁷.

Table1. Selected FT-IR absorption bands of ligand and its nano metal complexes.

Comp.	ν COOH	ν C=O	ν C-N ν N-C-N	ν N-H imidazole ring	ν CH ₂ - N	ν C=N	ν M-N	Others
L	1708	1627	1271	3203	2964	1552	----	----
PtL	1712	1631	1273	3200	2972	1543	462	ν (H ₂ O) = 3442 ν Pt-Cl = 352
AuL	1713	1618	1271	3211	2978	1547	459	ν (H ₂ O) = 3450 ν Au-Cl = 345

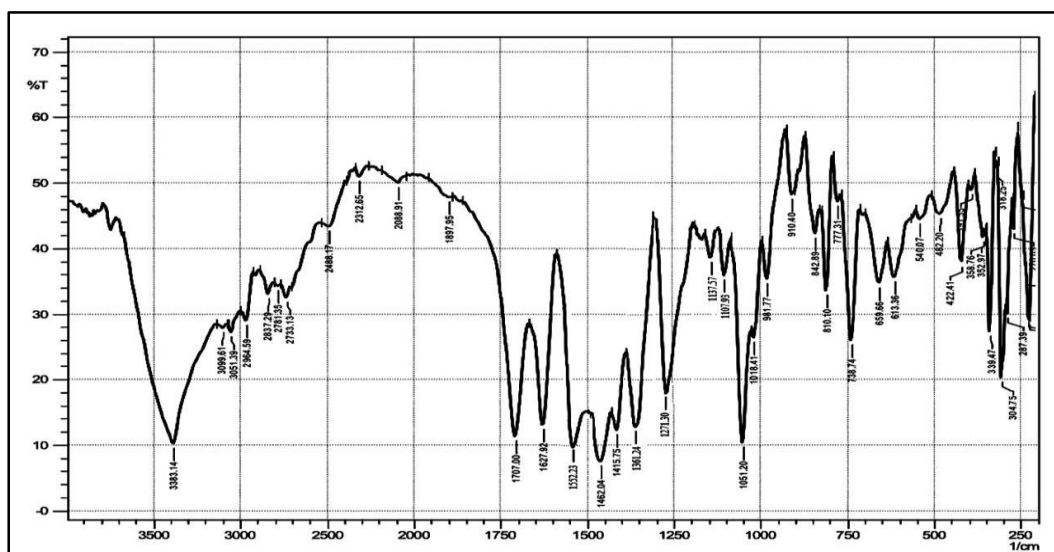


Figure1. FTIR spectrum of ligand.

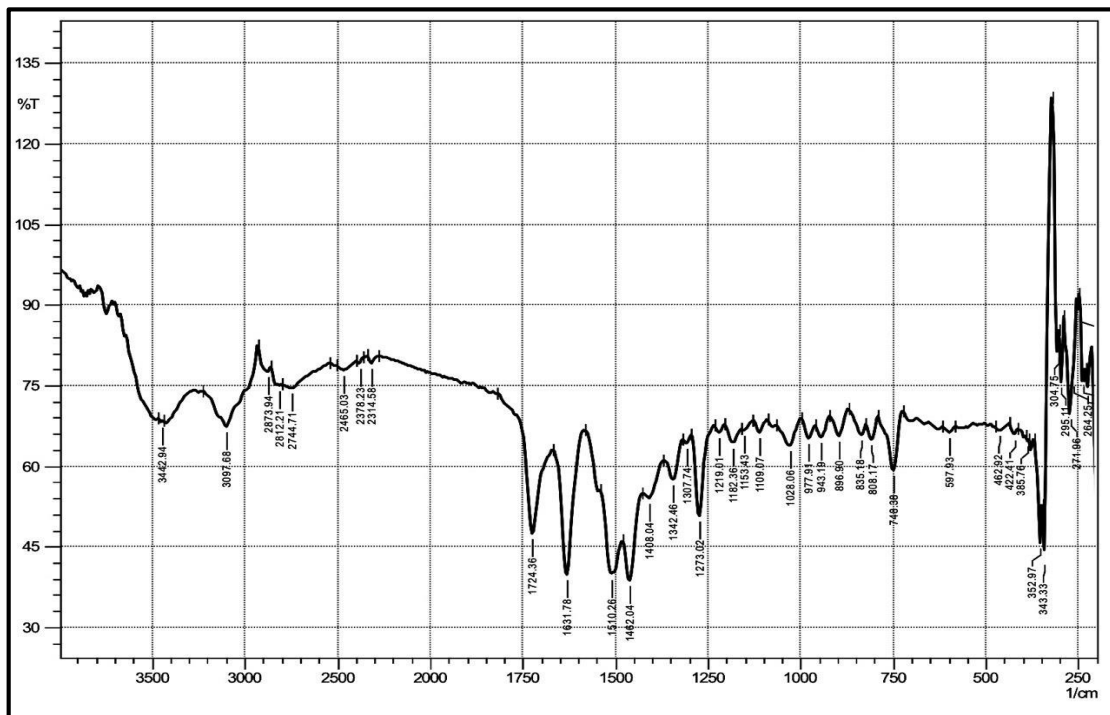


Figure 2. FTIR spectrum of Pt(IV)nanocomplex.

X-ray Diffraction Analysis

One of the important analytical techniques is the diffraction of X-ray from a crystal's planes or diffraction analysis. X-ray diffraction, which is dependent on the solid's crystal properties, allows us to determine the crystal structure of many different solid compounds by analyzing their structure. We can also determine the arrangement of molecules in crystal¹⁸ by using this method. XRD data was used to confirm the phase formation and calculate the particle size. Average particle size for different specimens was obtained from the main peaks using the Debye Scherrer equation¹⁹ Eq. 2:

$$D = k\lambda / \beta \cos\theta \quad \dots 2$$

Where D = crystallite size, k = shape factor = 0.9, θ = diffraction angle at maximum peak intensity. B = full width at half maximum of diffraction angle in radians. λ = x ray wavelength. Figure 3 displays the X-ray diffraction of a synthetic Pt nanocomplex. Pt nanocomplex exhibits the following X-ray diffraction patterns at 2θ values: (13.05, 17.11, 18.44, 24.06 and 27.78°). The X-ray

diffractogram of Au nanocomplex is shown in Fig. 4. The graph compares the index 2θ values for each peak. When the values are compared, it can be seen that there is good agreement between the 2θ and d numbers. According to Fig.4, the diffraction peaks at 2θ are (12.18, 13.81, 16.07, 17.42, 22.05, 25.59, and 27.81 °). The collected data suggest that the Au(III) nanocomplex is more crystalline than the Pt(IV) nanocomplex, which has an amorphous phase. The samples sharp diffraction peaks showed that our method may produce complex nanocrystals that are well-crystallized²⁰. Table 2 displays the X-ray diffraction data for nanocomplexes.

Table 2: X-ray diffraction data of nanocomplexes

NO	Complex	2θ	FWHM	d-spacing (Å)	Graine size (nm)
1	AuL	17.42	0.3936	10.74	21.33
2	PtL	13.05	0.2460	34.77	33.96

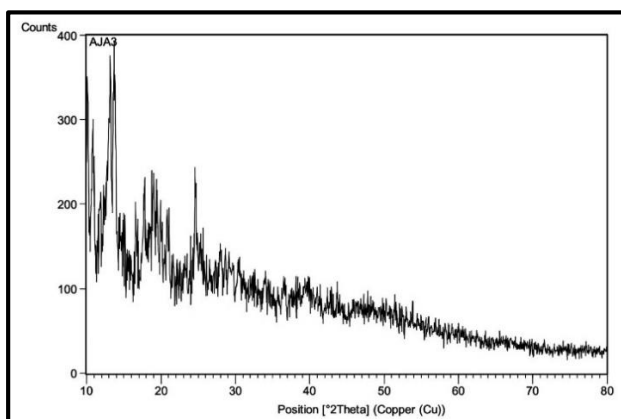


Figure 3. X-ray diffraction spectrum of Pt(IV) nanocomplex

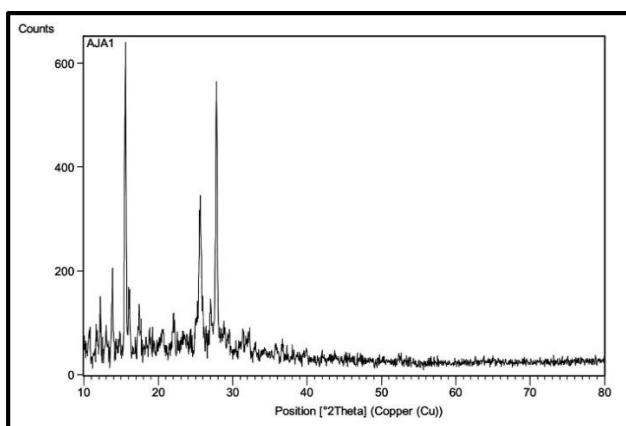


Figure 4. X-ray diffraction spectrum of Au(III) nanocomplex

Morphological Characterization:

Transmission Electron Microscope (TEM)

A transmission electron microscope was used to examine the morphological characteristics of the nanocomplex as it had been created. The Pt(IV) nanocomplex is depicted in Fig.5 as irregularly shaped, agglomerated nanoparticles that are 30 nm in size. Figure 6 depicts the transformation of the agglomerated, irregularly shaped nanoparticles into the primarily quasi-spherical morphology of the Au(III) nanocomplex. The XRD and TEM particle sizes were different²¹ because the XRD particle is the crystallized size or primary particle, which is a single crystal particle. A particle consisting of one, two, or even more primary particles is known as a TEM particle.

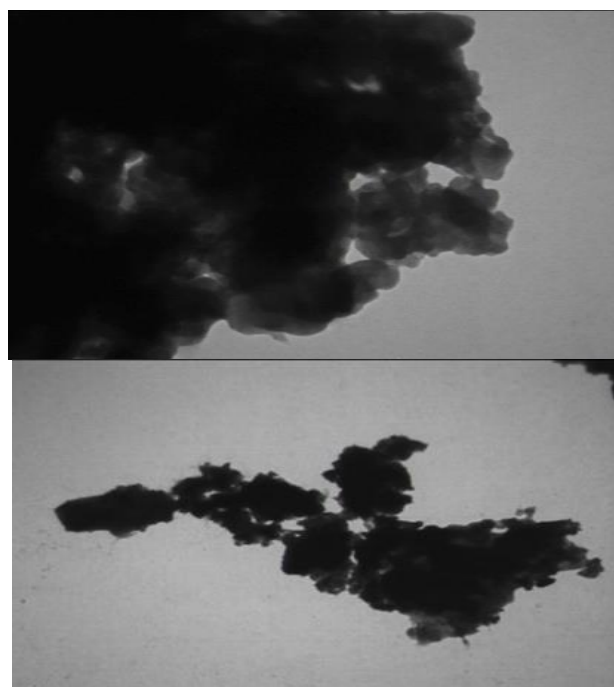


Figure 5. TEM image of Pt(IV) nanocomplex.

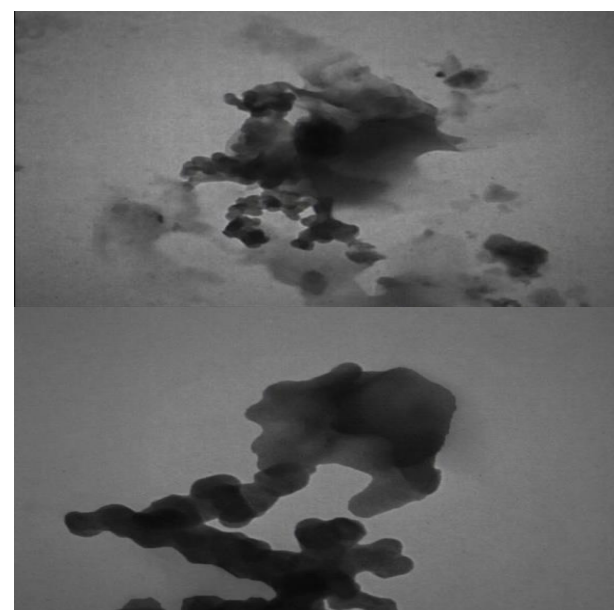


Figure 6. TEM image of Au(III) nanocomplex.

Energy Dispersive X-ray (EDX) Analysis

Energy dispersive X-ray (EDX) analysis was used to determine the composition of the synthesized nanocomplexes. The findings indicated that the proportion of experimental atoms is nearly in agreement with the predicted (theoretical) values. The characteristic signals for carbon, oxygen, chlorine, fluorine, sulfur, and platinum are noticeable in the EDX spectrum of the Pt(IV)

nanocomplex, whereas the characteristic signals for carbon, oxygen, chlorine, fluorine, sulfur, and gold are noticeable in the EDX spectrum of the Au(III) nanocomplex.

Field Emission Scanning Electron Microscopes (SEM)

Field emission scanning electron microscopes (SEM) were used to examine the shape, size, and structure of the nanomaterials²². The SEM images of the nanocomplexes for Pt(IV) and Au(III), respectively, are shown in Fig.7 and 8. The presence of a metal ion played a major role in how differently the nanocomplex was shaped. Pt(IV) nanocomplex particles were 20 nm in size on average, whereas Au(III) nanocomplex particles were 10–25 nm in size. The synthetic complex, which is the size of a nanoparticle, may be extremely helpful in a variety of areas, including biological and industrial applications.

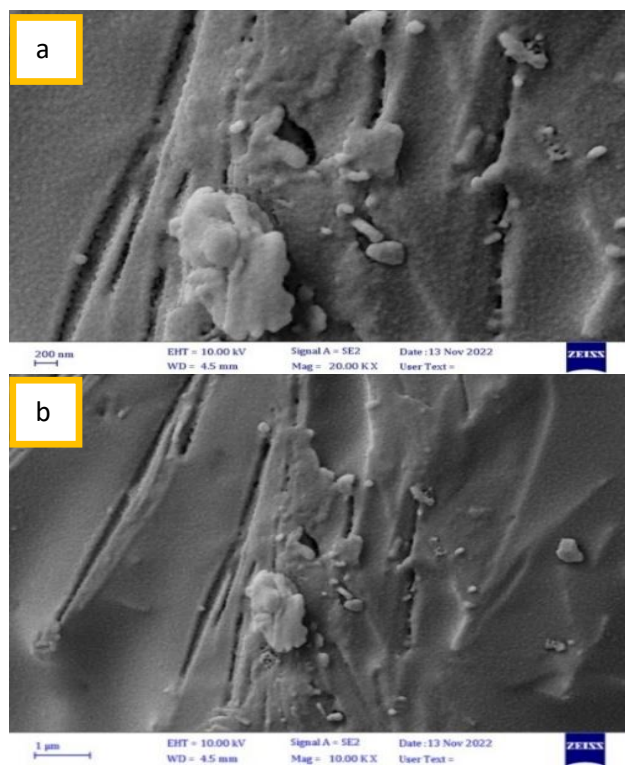


Figure 7 .FESEM image of Pt(IV) Complex(a:200nm and b: 1μm)

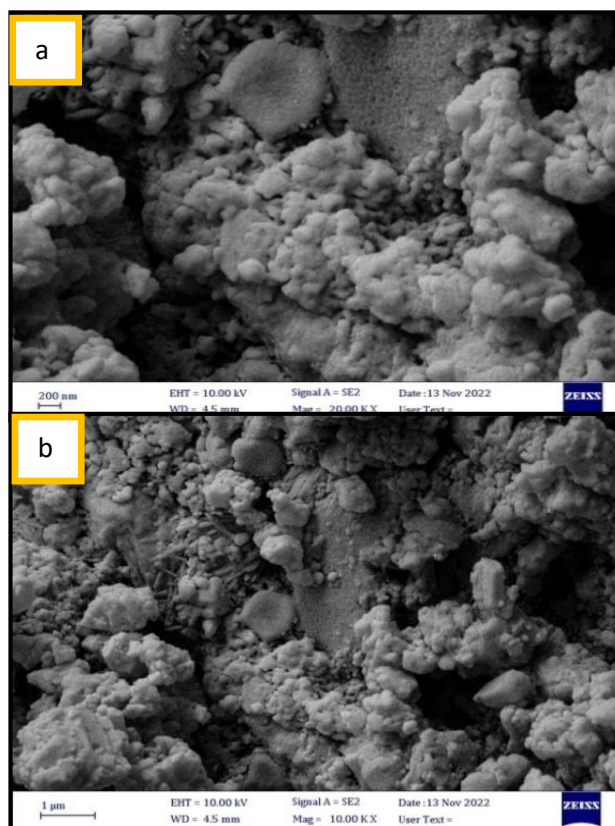


Figure 8. FESEM image of Au(III) Complex(a:200nm and b: 1μm).

Atomic Force Microscope (AFM)

The surface morphology and roughness of the produced nanoparticles have been characterized using the AFM. Figs. 9 and 10 respectively depict the two- and three-dimensional AFM images of the Pt(IV) and Au(III) nanocomplexes. According to the Figs., the obtained particle size distribution results for Pt(IV) and Au(III) nanocomplexes are in the range of 5-31 nm and 5-33 nm, respectively. The average diameter of the Pt(IV) nanocomplex was 17 nm, and Au(III) nanocomplex was 18 nm. This result demonstrates that these produced materials have nanoscale particles. The photos additionally display the great regularity of the surface objects which is a real reflection of the surface organization of Pt(IV) and Au(III) nanocomplexes.

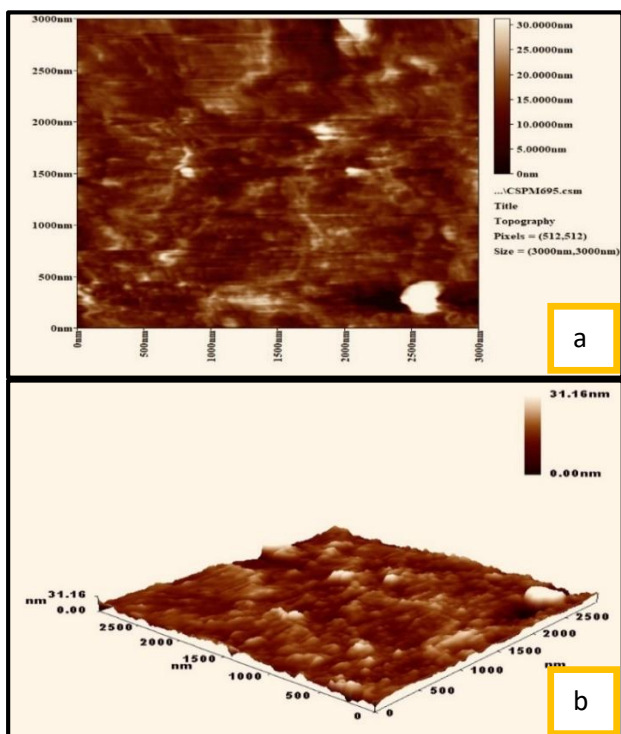


Figure 9. AFM image of Pt(IV) nanocomplex (a: two dimensional, b: three dimensional).

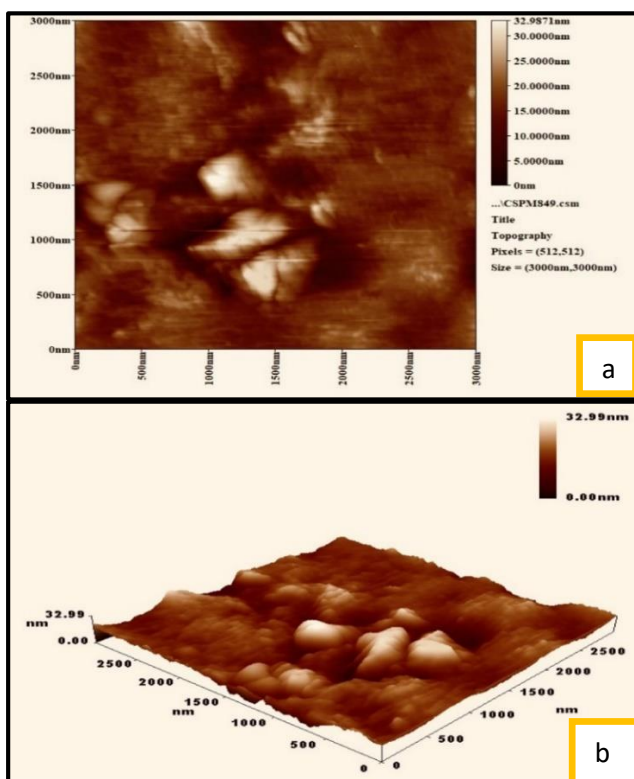


Figure 10. AFM image of Au(III) nanocomplex (a: two dimensional, b: three dimensional).

Antioxidant Activity

The DPPH (Diphenyl-1-picrylhydrazyl) technique was used to assess the synthesized compound's antioxidant activity. The DPPH reagent's change from purple to yellow serves as a marker for the ability of synthetic compounds to scavenge free radicals^{23, 24}. Standards were ascorbic acids. The antioxidant potential of the molecule was initially evaluated at 6.25, 12.5, 25, 50, and 100 $\mu\text{g/ml}$. All of the synthesized compounds exhibited good to excellent action against the DPPH free radical. The Au(III) nanocomplexes increased the percentage of scavenging activity while the free ligands displayed low DPPH activity, indicating that the metal nano complexes have greater scavenging activity than the ligands. In comparison to the ligand and Pt(IV) nanocomplexes, Au(III) nano complexes at (100 $\mu\text{g/ml}$) demonstrated a higher radical scavenging percentage. As the inhibitory concentrations (IC₅₀) values decrease, the percentage of ligand and metal nanocomplexes having scavenging action increases. Table 3 and Fig. 11 demonstrate the ligand and its nanocomplexes scavenging activity.

Table3. Scavenging activity of the ligand and their nanocomplexes.

Comp.	Scavenging %					Ic50
	6.25 µg/ml	12.5 µg/ml	25 µg/ml	50 µg/ml	100 µg/ml	
Ligand	14.41	27.76	39.92	39.6	51.99	85.85
Pt(IV) nanocomplex	18.23	22.09	22.89	31.11	45.73	12.94
Au(III) nanocomplex	35.31	48.76	52.12	69.7	91.89	115.55
Ascorbic acid	41.4	50.4	67.1	71.7	97.2	10.21

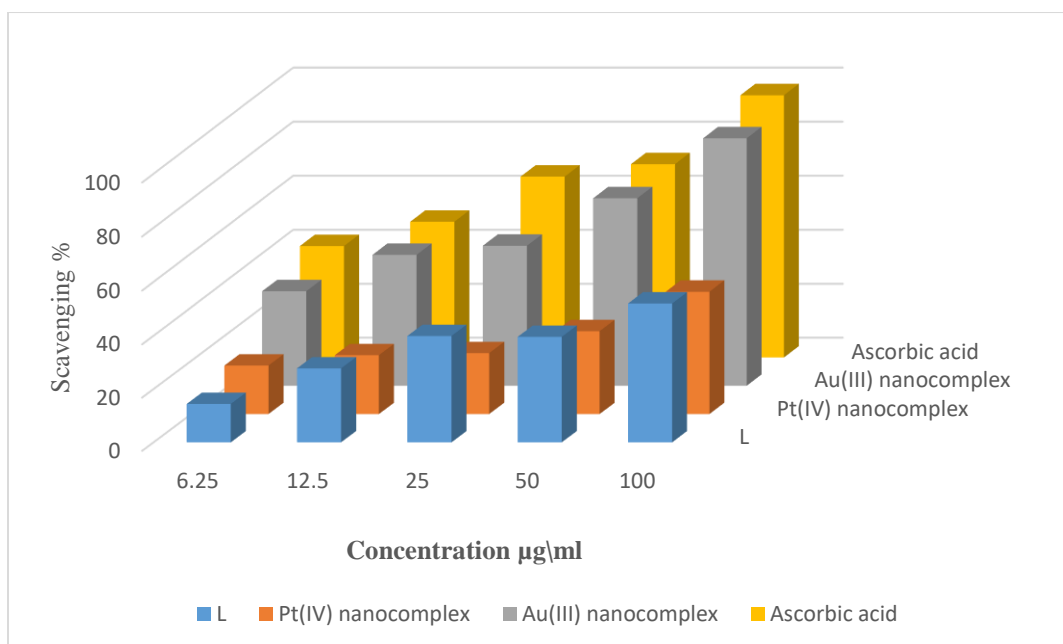


Figure 11. IC50 values of DPPH scavenging activity of the ligand and its nanocomplex.

Conclusion

In conclusion, the study described the synthesis and spectroscopic characterization of Pt(IV) and Au(III) complexes with a novel Mannich base ligand synthesized by condensation of ciprofloxacin with 2-mercaptobenzimidazole. Nanocomplexes synthesis have been by using the ultrasonic sonication method. Our method displayed that the nanocomplex may be made easily and without aggregation. The complexes were characterized by transmission electron microscopy (TEM), atomic force microscopy (AFM), energy dispersive X-ray (EDX), scanning electron microscopy (SEM), x-ray diffraction (XRD), and Fourier Transform Infrared Spectroscopy (FTIR). According to the study's finding, nanocomplexes should have particle sizes

between 17 and 20 nm. The Au(III) nanocomplex showed high activity, the IC₅₀ value of this complex was (12.94 µg/ml), which was lower than the value for the ascorbic acid standard compound (10.21 g/ml), and the ligand showed moderate activity compared to the Pt(IV) nanocomplex's weak antioxidant activity. The IC₅₀ values for the ligand and pt(IV) nanocomplex conjugate were 85.85 g/ml and 115.55 g/ml, respectively. All compounds exhibited low activity when compared to ascorbic acid. The nanocomplexes that may be created for use as antioxidant applications. These inorganic nanocomplexes could be used in a number of different fields.

Acknowledgment

We thank the University of Baghdad for technical support.

Authors' Declaration

- Conflicts of Interest: None.
- We hereby confirm that all the Figures and Tables in the manuscript are ours. Furthermore, any Figures and images, that are not ours, have been included with the necessary permission for re-publication, which is attached to the manuscript.
- Authors sign on ethical consideration's approval
- Ethical Clearance: The project was approved by the local ethical committee at University of Baghdad.

Authors' Contribution Statement

A.J.A, made the conception, design, acquisition of data signature. M.F.A did the analysis, interpretation, drafting the MS, revision and proofreading.

References

1. Halliwell B, Gutteridge JMC. Free Radicals in Biology and Medicine, 4th ed.; Halliwell, B., Gutteridge, J.M.C., Eds.; Oxford University Press: New York, NY, USA, 2007.
<https://doi.org/10.1093/acprof:oso/9780198717478.01.0001>.
2. Tena N, Martín J, Asuero A G. State of the art of anthocyanins: Antioxidant activity, sources, bioavailability, and therapeutic effect in human health. *Antioxidants*. 2020; 9(5): 451.
<https://doi.org/10.3390/antiox9050451>.
3. Onwudiwe D C, Ekennia A C. Synthesis, characterization, thermal, antimicrobial and antioxidant studies of some transition metal dithiocarbamates. *Res Chem Intermed*. 2017; 43(3): 1465-1485. <https://doi.org/10.1007/s11164-016-2709-2>.
4. Joshi S, Bilgaiyan P, Pathak A. Synthesis, spectroscopic characterization and antibacterial screening of novel Mannich bases of Ganciclovir. *Arab J Chem*. 2017; 10: 1180-1187. S1180-S1187.
<https://doi.org/10.1016/j.arabjc.2013.02.013>.
5. Kerru N, Gummi L, Maddila S, Gangu K K, Jonnalagadda SBA. review on recent advances in nitrogen-containing molecules and their biological applications. *Molecules*. 2020; 25(8): 1909.
<https://doi.org/10.3390/molecules25081909>.
6. Ebenezer O, Jordaan M A, Carena G, Bono T, Shapi M, Tuszynski J A. An Overview of the Biological Evaluation of Selected Nitrogen-Containing Heterocycle Medicinal Chemistry Compounds. *Int J Mol Sci*. 2022; 23(15): 8117.
<https://doi.org/10.3390/ijms23158117>.
7. Sankar A, Balakrishnan A . Aminomethylation, Structure and Biological activity of the new Mannich base and its Transition metal Complexes Derived from Isoindole-1, 3 (2H)-dione .*Chem Sci Rev Lett*. 2019; 8(29): 16-21.
<https://doi.org/10.24996/ijcs.2022.63.12.1>.
8. Abu-Dief A M, El-Metwaly N M, Alzahrani S O, Alkhatib F, Abualnaja M M, El-Dabea T, et al . Synthesis and characterization of Fe (III), Pd (II) and Cu (II)-thiazole complexes; DFT, pharmacophore modeling, in-vitro assay and DNA binding studies. *J Mol Liq*. 2021; 326: 115277.
<https://doi.org/10.1016/j.molliq.2021.115277>.
9. Abou-Melh KS, Al-Hazmi GA, Althagafi I, Alharbi A, Shaaban F, El-Metwaly NM, et al. Synthesis, characterization, DFT calculation, DNA binding and antimicrobial activities of metal complexes of dimedone arylhydrazones. *J Mol Liq*. 2021; 334: 116498.
<https://doi.org/10.1016/j.molliq.2021.116498>.
10. Eftekhari A, Ahmadian E, Azami A, Johari-Ahar M, Eghbal MA. Protective effects of coenzyme q10 nanoparticles on dichlorvos-induced hepatotoxicity and mitochondrial/lysosomal injury. *Environ Toxicol*. 2018; 33: 167–177. <https://doi.org/10.1002/tox.22505>.
11. Pohlmann AR, Schaffazick SR, Creczynski-Pasa TB, Guterres SS. Preparation of drug-loaded polymeric nanoparticles and evaluation of the antioxidant activity against lipid peroxidation. In *Free Radicals and Antioxidant* . *Methods Mol Biol*. 2010; 610: 109–121.
https://doi.org/10.1007/978-1-60327-029-8_7.
12. Feng L S, Liu M L, Zhang S, Chai Y, Wan B, Zhang Y B, et al. Synthesis and in vitro antimicrobial activity of 8-OCH₃ ciprofloxacin methylene and ethylene isatin derivatives. *Eur. J. Med. Chem* . 2011; 46(1): 341-348.
<https://doi.org/10.1016/j.ejmech.2010.11.023>.
13. Öztürk İ, Beğic N, Bener M, Apak R. Antioxidant capacity measurement based on κ-carrageenan stabilized and capped silver nanoparticles using green nanotechnology. *J. Mol. Struct*. 2021; 1242: 130846.
<https://doi.org/10.1016/j.molstruc.2021.130846>.
14. Kumar J, Kumar N, Sati N, Hota P K. Antioxidant properties of ethenyl indole: DPPH assay and TDDFT studies. *New J. Chem*. 2020; 44(21): 8960-8970.
<https://doi.org/10.1039/D0NJ01317J>.

15. Abdulameer J H, Alias M F. Heavy Metal Complexes of 1, 2, 3-Triazole derivative: Synthesis, Characterization, and Cytotoxicity Appraisal Against Breast Cancer Cell Lines (MDA-MB-231). *Baghdad Sci. J.* 2022; 19(6): 1410-1422. <https://doi.org/10.21123/bsj.2022.7178>.
16. Mahmood Z N, Alias M, El-Hiti GAR, Ahmed DS, Yousif E. Synthesis and use of new porous metal complexes containing a fusidate moiety as gas storage media. *Korean J. Chem. Eng.* 2021;38: 179-186. <https://doi.org/10.1007/s11814-020-0692-1>.
17. Kowalczyk D, Gładysz A, Pitucha M, Kamiński D M, Barańska A, Drop B. Spectroscopic Study of the Molecular Structure of the New Hybrid with a Potential Two-Way Antibacterial Effect. *Molecules.* 2021;26(5): 1442. doi. <https://doi.org/10.3390/molecules26051442>.
18. Ali A, Chiang Y W, Santos R M. X-ray diffraction techniques for mineral characterization: A review for engineers of the fundamentals, applications, and research directions. *Minerals.* 2022; 12(2): 205. <https://doi.org/10.3390/min12020205>.
19. Baqer S R, Alsammarraie A M A, Alias M, Al-Halbosi M M, Sadiq A S. In Vitro Cytotoxicity Study of Pt Nanoparticles Decorated TiO₂ Nanotube Array. *Cancer.* 2020;17(4): 1169-1176. <https://doi.org/10.21123/bsj.2020.17.4.1169>
20. Podorov S G, Faleev N N, Pavlov K M, Paganin D M, Stepanov S A, Förster E. A new approach to wide-angle dynamical X-ray diffraction by deformed crystals. *J. Appl. Crystallogr.* 2006;39(5): 652-655. <https://doi.org/10.1107/S0021889806025696>.
21. Sagadevan S, Koteeswari P. Analysis of structure, surface morphology, optical and electrical properties of copper nanoparticles. *J. Nanomed. Res.*, 2015;2(5): 00040-00048. <https://doi.org/10.3390/nano10091812>.
22. Lewczuk B, Szyryńska N. Field-emission scanning electron microscope as a tool for large-area and large-volume ultrastructural studies. *Animals.* 2021 ;11(12): 3390. <https://doi.org/10.3390/ani11123390>.
23. Higgins MR, Izadi A, Kaviani M. Antioxidants and exercise performance: with a focus on vitamin E and C supplementation. *I J E R P H.*2020; 17(22): 8452. <https://doi.org/10.3390/ijerph17228452>.
24. Baliyan S, Mukherjee R, Priyadarshini A, Vibhuti A, Gupta A, Pandey R P, et al. Determination of antioxidants by DPPH radical scavenging activity and quantitative phytochemical analysis of *Ficus religiosa*. *Molecules.*2022; 27(4): 1326. <https://doi.org/10.3390/molecules27041326>.

تحضير ، تشخيص طيفي ، دراسة التراكيب لمعقدات أيونات البلاتين ⁴⁺ و الذهب ³⁺ النانوية مع ليكاند قاعدة مانخ و تقييم نشاطها كمضادات للاكسدة

علياء جبار احمد¹ ، محاسن فيصل احمد²

¹وزارة التعليم العالي و البحث العلمي ، بغداد ، العراق.

²قسم الكيمياء ، كلية العلوم للبنات ، جامعة بغداد ، بغداد ، العراق.

الخلاصة

في هذا البحث تم تحضير المركبات المعدنية النانوية الجديدة لأيونات البلاتين ⁴⁺ و الذهب ³⁺ مع ليكاند قاعدة مانخ جديد مشتق من السبيروفلوكسامين بطريقة الموجات فوق الصوتية. تم تشخيص المعقدات النانوية والليكاند الجديد باستخدام تقنيات فيزيائية و كيميائية مختلفة مثل أطياف الأشعة تحت الحمراء، حيود الأشعة السينية، المجهر الإلكتروني الماسح، المجهر الإلكتروني النافذ و مجهر القوة الذرية. تم تحديد نشاط مضادات الأكسدة لدى الليكاند و معقداته النانوية. أظهرت النتائج أن المعقدات النانوية واعدة أكثر بأن تستخدم كمضادات للاكسدة في المستقبل خاصة عند التراكيز العالية

الكلمات المفتاحية: مضادات الاكسدة ، سبيروفلوكسامين ، جذور حرة ، معقدات قاعدة مانخ ، حجم نانوي.